

MODELLING OF THE LUBRICANT-LAYER THICKNESS ON A MANDREL DURING ROLLING SEAMLESS TUBINGS

MODELIRANJE DEBELINE PLASTI MAZIVA NA TRNU PRI VALJANJU BREŽŠIVNIH CEVI

Dušan Čurčija, Ilija Mamuzić

Croatian Metallurgical Society, Berislavićeva 6, Zagreb, Croatia
ilija.mamuzic@public.carnet.hr

Prejem rokopisa – received: 2012-07-03; sprejem za objavo – accepted for publication: 2013-02-26

AutoCAD-a 3D modelling and the programs of Mathematica, MATLAB and MathCAD Professional were used to calculate the approximate solutions of the Reynolds differential equations for lubrication. Excel Software and Monte-Carlo solutions are compared. The results indicate a fast decrease in the lubricant-layer thickness in the stands for the continuous rolling of tubes. At the start of the rolling, the conditions for stable hydrodynamic lubrication are fulfilled for the tube-diameter-reduction processes. Theoretical calculations indicate that, on the finishing stands, "lubricant pickling" may occur on the mandrel. An approximate calculation is performed for the rolling point M and verified with the numerical Monte-Carlo method.

Keywords: Reynolds equation, AutoCad camera viewing, lubricant, continuous rolling line, seamless tubes

Za izračun približnih rešitev Reynoldsovih diferencialnih enačb za mazanje so bili uporabljeni modeliranje AutoCAD-a 3D in programi Mathematica, MATLAB in MathCAD Professional. Primerjane so rešitve, dobljene s programom Excel in z numerično metodo Monte-Carlo. Rezultati kažejo hitro zmanjšanje debeline plasti maziva na ogrodjih za kontinuirno valjanje cevi. Na začetku valjanja, pri postopku zmanjševanja premera cevi, so izpolnjeni pogoji za stabilno hidrodinamsko mazanje. Teoretični izračuni kažejo, da lahko pri končnih ogrodjih na trnu pride do odsotnosti mazanja. Izvršen je približen izračun pri točki valjanja M, ki je bil preverjen z numerično metodo Monte-Carlo.

Ključne besede: Reynoldsova enačba, opazovanje z AutoCad-kamero, mazivo, kontinuirna valjarniška linija, brezšivne cevi

1 INTRODUCTION

Tube rolling with round calibres¹ is a variant of longitudinal rolling with a formation of a deformation zone and in **Figure 1** the rolls and a mandrel are shown. The tubes rolling on a long floating mandrel use rolling lines with 7 to 9 working stands. Before inserting the rolling stock between the rolls, a cylindrical mandrel is

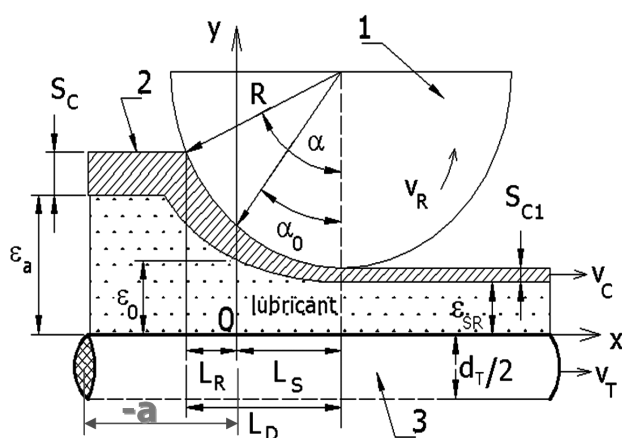


Figure 1: Scheme of rolling seamless tubes on a continuous rolling line

Slika 1: Shema valjanja brezšivnih cevi na kontinuirni valjarniški progi

put in, which then moves in the deformation zone jointly with the rolled tube. At the exit from the rolls, the mandrel speed is lower than that in the front tube part. The characteristic of the rolling is that the speeds of the tube and rolls are equal in the deformation zone only in two points of the roll groove. In recent years continuous rolling processes with a deformation of tubes with a stable, long, cylindrical cone mandrel or step-shaped mandrel were developed. The characteristic of this rolling is that there are two subzones of the reduction of the tube diameter and of the tube wall thickness, as shown in **Figure 1**. On the exterior contact of the tube and the rolls^{2,3} without a lubricant addition, friction occurs according to Kulon-Amonton laws, while in the tube interior, because of the lubricant presence, Newton's laws of fluid friction govern. The extent of the tangential stresses in the lubricant layer^{4,5} is calculated from equation (1):

$$\tau_x = \frac{\mu(v_C - v_T)}{\varepsilon(x)} - \frac{1}{2}\varepsilon(x)\frac{\partial p}{\partial x} \quad (1)$$

The change in the pressure in the lubricant layer⁴⁻⁷ is calculated from equation (2) and the volume of the lubricant used on the tube perimeter^{6,7} from equation (3):

$$\frac{dp}{dx} = \frac{6\mu(v_C + v_T)}{\varepsilon^2(x)} - \frac{12\mu Q}{\varepsilon^3(x)} \quad (2)$$

$$Q(x) = \int_0^{\varepsilon(x)} u dy = \frac{1}{12\mu} \frac{dp}{dx} \varepsilon^3(x) + \frac{(v_c + v_T)}{2} \varepsilon(x) \quad (3)$$

The geometry of the lubricant contact⁸⁻¹⁰ is calculated from equation (4) and the lubricant wedge length from equation (5):

$$\varepsilon(x) = \varepsilon_0 + R_0 \left[\cos \alpha_0 - \sqrt{1 - \left(\sin \alpha_0 - \frac{x}{R_0} \right)^2} \right] \quad (4)$$

$$a = R_0 \left[\sqrt{1 - \left(\cos \alpha_0 - \frac{\varepsilon_a}{R_0} + \frac{\varepsilon_0}{R_0} \right)^2} - \sin \alpha_0 \right] \quad (5)$$

$$\varepsilon(x) = \varepsilon_0 - \alpha_0 x + \frac{x^2}{2R_0} - \frac{\alpha_0 x^2}{2R_0^2} + \frac{x^4}{8R_0^3} \quad (6)$$

Relation (6) is an evolution¹¹⁻¹³ of equation (4) in a Maclaurin series. The lubricant characteristic for the theoretical investigation and the process geometry used are quoted from the references^{8,11} and are shown below.

The scheme of the tube-wall deformation geometry is shown in **Figure 2**. The cone shape of the tube is representative of the continuous rolling-line outset.

2 DISCUSSION, SOLUTIONS AND GRAPHIC INTERPRETATION

The equations for the approximate analytical solutions are listed in **Table 1**. The solution for the Ψ range is achieved using the gripping angle α from references^{11,14}, being the known solution of Grudev, Mazur and Kolmogorov¹⁴.

The solutions for the Ω range, M point and $\Phi\Sigma$ are derived in this work.

Figure 3 represents a comprehensive understanding of the solutions from **Table 1**. The M point is shown in a set of relations $\{\varepsilon_a^{1/3}; \Delta\varepsilon_0/\varepsilon_a\}$. For series 1, $\Delta\varepsilon_0$ is the difference from the pilot ε_0^1 , i.e., the lubricant-layer thickness for every gripping α angle, minus the lubricant layer thickness for the pilot at 0.1 rad. Similarly, series 2

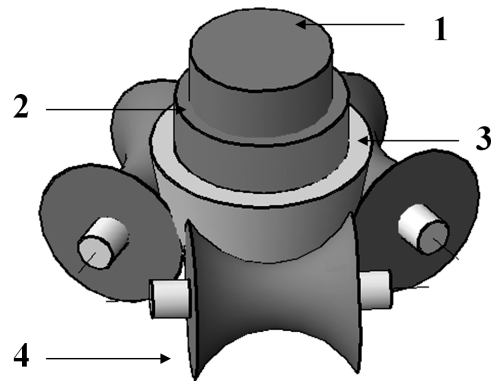


Figure 2: Stand with three rolls used in the analysis of tribomechanical systems: 1- mandrel, 2- lubricant, 3- tube, 4- roll

Slika 2: Ogradnje s tremi valji, uporabljeno pri analizi tribomehanskih sistemov: 1- trn, 2- mazivo, 3- cev, 4- valj

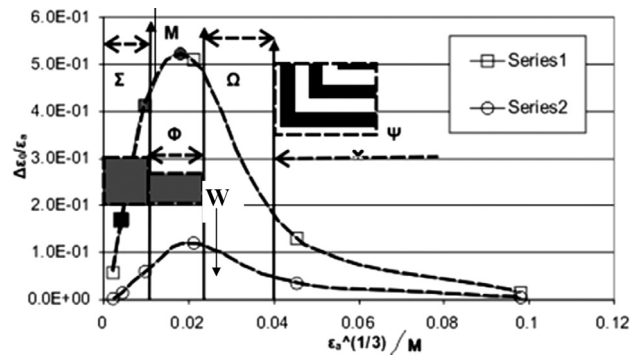


Figure 3: Distribution of the areas along the rolling line according to the solutions from **Table 1**

Slika 3: Porazdelitev področij po dolžini valjarniške proge skladno z rešitvami v tabeli 1

is calculated for $\varepsilon_0^1 - \varepsilon_0^* / \varepsilon_a$ and pilot ε_0^1 , with ε_0^* as the variable thickness of the lubricant layer.

Figure 4 shows a model of the lubricant layer on the mandrel calculated using the numerical Monte-Carlo method. At the entry (I) the lubricant is in surplus, while, at the exit of the continuous rolling line (II), the lubricant layer on the mandrel is picked because of the absence of fresh lubricant.

Table 1: Approximate solutions of equation (2)

Tabela 1: Približne rešitve enačbe (2)

Zone of Fig. 3	Approximate analytical solution
Ψ	$\varepsilon_0^* = 0.7726\varepsilon_0^1 \quad \varepsilon_0^* = 0.5R_0(\alpha^*)^2 \quad \alpha^* = \sqrt[3]{\frac{8}{15R_0A}} \quad \varepsilon_a \gg \varepsilon_0$
Ω	$\alpha^* = 2 \cdot \sqrt[3]{\frac{\varepsilon_a \sqrt{2R_0\varepsilon_a}}{10R_0^2 + 15R_0^2 A \varepsilon_a \sqrt{2R_0\varepsilon_a}}} \quad \varepsilon_0^* = \frac{R_0(\alpha^*)^2}{2}$
M point	$\alpha_0^* = \left(\frac{2}{5}\right)^2 \frac{1}{A\varepsilon_{aMAX}} \quad \varepsilon_0^* = \frac{R_0(\alpha_0^*)^2}{2} \quad \varepsilon_{aMAX} = 0.28674 \cdot \sqrt[3]{\frac{R_0}{A^2}}$
Φ Σ	$\varepsilon_0^1 = \varepsilon_a \left(1 - \frac{0.57348\varepsilon_a}{\varepsilon_{aMAX}}\right) \quad \varepsilon_{aMAX} = 0.28674 \cdot \sqrt[3]{\frac{R_0}{A^2}} \quad \varepsilon_a \rightarrow \varepsilon_0$

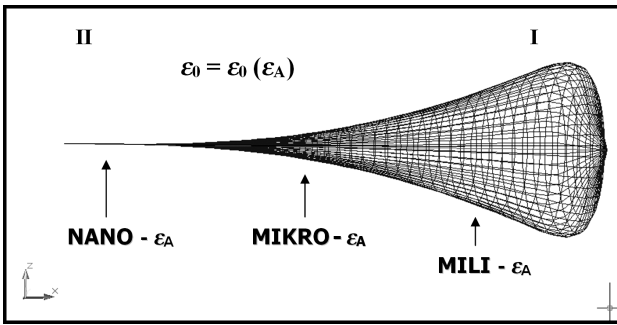


Figure 4: AutoCAD modelled lubricant layer on the mandrel along the rolling line

Slika 4: AutoCAD modelirana plast maziva na trnu po dolžini valjarniške proge

In Figure 5 approximate analytical solutions and numerical calculations are compared. Series 1 relates to the Φ area; series 2 relates to the Σ area, the marker of square M is the solution for the M point from Table 1; series 3 is the Monte-Carlo solution and numbers 1, 2, 3 and 4 indicate the positions of the AutoCAD viewing

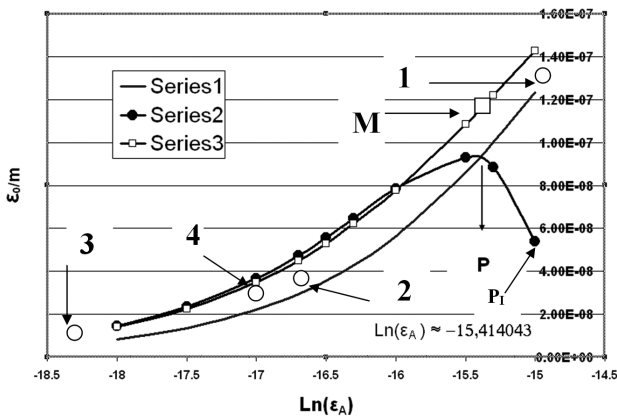


Figure 5: Comparison of the approximate analytical solutions from Table 1 and numerical Monte-Carlo solutions for the area between the approximate center of the rolling line and the exit stands

Slika 5: Primerjava približnih analitičnih rešitev iz tabele 1 in numeričnih rešitev Monte-Carlo za področje od približno sredine valjarniške proge do končnih ogrodij

Table 2: 3D cameras for Figure 6, viewing left to W on Figure 5

Tabela 2: 3D-kamere za sliko 6, pogled levo od W na slici 5

Figure	Marking	Remark
Common markings		
Fig. 6 Fig. 7	Mark 1	Ω - area in Figure 3 and Table 1
	Mark 2	Σ - area in Figure 3 and Table 1
	Mark 3	Numerical Monte-Carlo method
	Mark 4	Point M in Figure 3, mark M in Figure 5, point M in Table 1
	$Ln(\epsilon_A)$, $Ln(\epsilon_0)$	Abscissa and ordinate in 2D, for the AutoCAD command Revsurf
Specific markings		
Figure	Marking	Remark
Fig. 6	Markers 1, 4	"Hat" obtained with the rotation of the arc P-P ₁ in Figure 5
Fig. 7	P	Drawing of pyramid for point P in Figure 3 (cross-section of Ω and Σ)

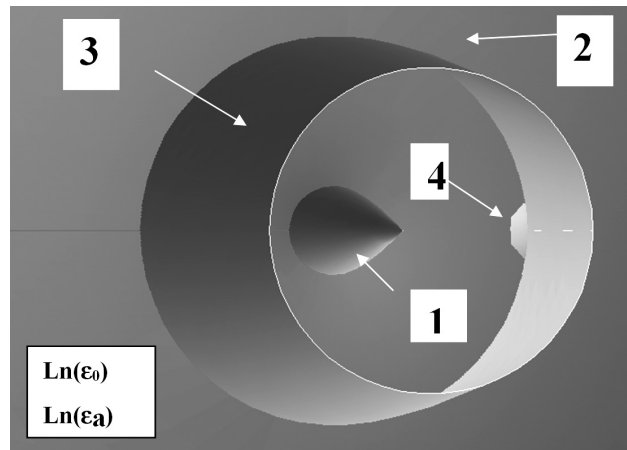


Figure 6: Viewing position 1 from Figure 5. The camera is covering the area between the center and the exit of the rolling line.

Slika 6: Pogled s pozicije 1 na slici 5. Kamera obsega področje od sredine do konca valjarniške proge.

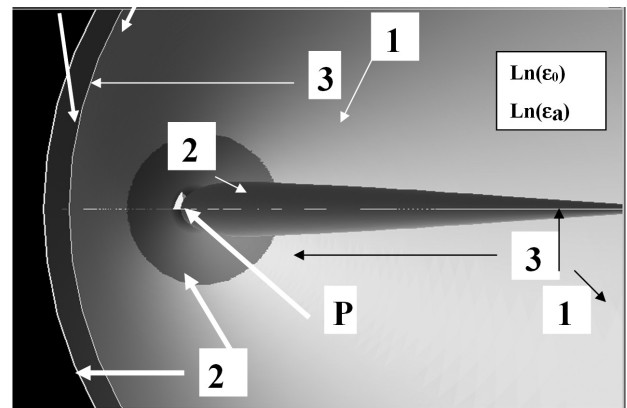


Figure 7: Viewing point 4 from Figure 5. The camera is directed to the approximate analytical solutions from Table 1.

Slika 7: Pogled s točke 4 na slici 5. Kamera je usmerjena k približnim analitičnim rešitvam v tabeli 1.

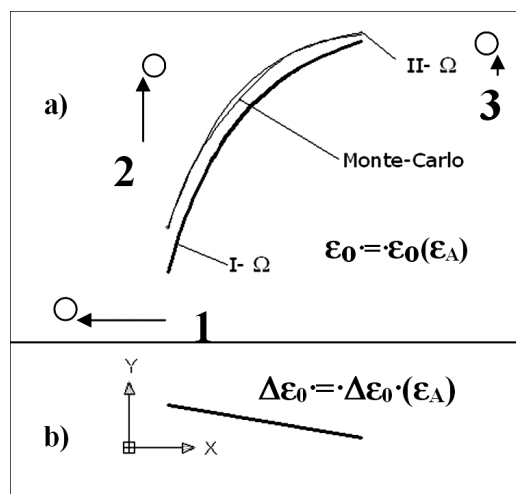


Figure 8: Comparison of the analytical and Monte-Carlo solutions for the area between the entering stands and the approximate center of the rolling line

Slika 8: Primerjava analitičnih rešitev in rešitev Monte-Carlo za področje od vhodnih ogrodij do približno sredine valjarniške proge

Table 3: Explanations of the markers from **Figure 9**

Tabela 3: Pojasnila k markerjem na **sliki 9**

Marker	Link	Remark
Series 1	Monte-Carlo	Numerical calculations
Series 2	Ω - area in Table 1	
Series 3	Solution according to M point in Table 1	Control of Monte-Carlo
Series 4	Σ - area in Table 1 , left of point P	Graph agrees with Monte-Carlo
Point P	Equal significance as in Figure 7	Cross-section of solutions Ω and Σ
Ω -I	The transition area around the M point where Ω no longer agrees with Monte-Carlo and Σ formula is not yet in accord with the Monte-Carlo solution. Acceptable for interpolations of the polygonal method. ¹⁴ In the interval, the section point P is a polynomial of degree 12.	

Table 4: Comparison of the approximate analytical solutions from **Table 1** with the numerical Monte-Carlo solution from around the middle to the exit of the rolling line

Tabela 4: Primerjava približnih analitičnih rešitev v **tabeli 1** z Monte-Carlo numerično metodo, od približno sredine valjarniške proge do izhodnih ogrođij

ε_a/m	Monte-Carlo ε_0^*/m	Zone Ω ε_0^*/m	M point ε_0^*/m	Zone Φ and Σ ε_0^*/m
9.420E-04	1.225E-05	1.225E-05	–	–
8.735E-05	1.136E-05	1.129E-05	–	–
1.069E-05	5.801E-06	–	5.801E-06	–
7.425E-06	4.618E-06	–	–	4.466E-06

cameras. According to solution Σ , $\ln(\varepsilon_A) \approx -15.414043$ for $\varepsilon_0 \rightarrow 0$.

The explanation of **Figures 6 and 7** is given in **Table 2**.

The numerical Monte-Carlo method and approximate analytical solutions for about half of the rolling line, according to references 7–9, are shown in **Figure 8**, where the calculated lubricant-layer thickness is shown for the area from the middle part to the exit of the rolling line. The linear correction of the Ω area was obtained with a solution in the M point according to **Table 1** and is also shown in **Figure 8b**.

An integral comparison for the whole continuous line is shown in **Figure 9** and, accordingly, for the abscissa as well in **Figure 5**. The markers are explained in **Table 3**.

An important characteristic of the M point is the control of the Monte-Carlo numerical method in this

point. The conditions from **Figure 9** are shown in **Table 4**.¹⁵

The solution for the M point has been confirmed. The numerical methods should be controlled in a narrow interval, at least in one initial point, with the approximate analytical solutions. In the case of the approximate analytical solutions with simplified mathematical solutions, the numerical methods are not reliable.

3 CONCLUSION

It is shown in several figures that the approximate analytical solutions of equation (2) from **Table 1** are in accordance with the numerical Monte-Carlo solutions. The representations in AutoCAD provide a refined understanding and a comparison, giving also realistic images of the lubricant on the mandrel for rolling the seamless tubes on a continuous line with several stands.

The solution developed for the M point^{15,16} is of special importance since it enables a linear correction of the lubricant layer in the area of the Ω formula and the correction can also be extended to the area Ω -I.

4 SYMBOLS

Symbol	Unit	Description
ε_0	m	Lubricant thickness in the entry section of the deformation zone (Figure 1)
ε_0^1	m	Lubricant thickness for the gripping angle α_0 tending to zero
$\varepsilon_0^{0.1}$	m	Lubricant-layer thickness for the gripping angle 0.1 rad, Figure 3 (series 1)

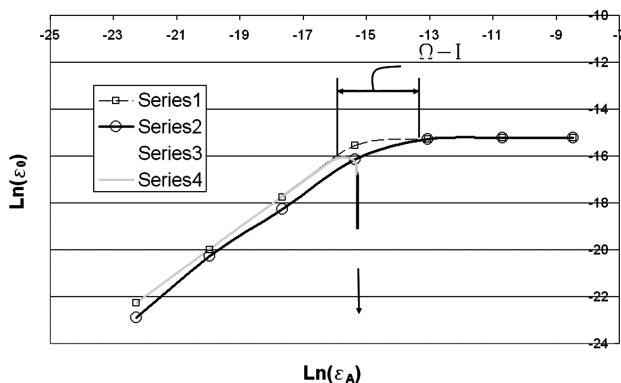



Figure 9: Comparison of the analytical solutions from **Table 1** with the numerical Monte-Carlo solutions for the whole rolling line

Slika 9: Primerjava analitičnih rešitev iz **tabele 1** in numeričnih rešitev Monte-Carlo vzdolž cele valjarniške proge

ε^*_0	m	Characteristic lubricant thickness for the square trinomial in relation (6), with zero as a discriminant of the square equation
$\varepsilon(x)$	m	Lubricant-layer thickness in the range $[-a : 0]$, Figure 1 , equation (4)
ε_{SR}	m	Average mandrel-lubricant thickness after a pass
ε_a	m	Lubricant-layer thickness on the mandrel after the entry section of the deformation zone
ε_{aMAX}	m	Characteristic lubricant-layer thickness on the mandrel in point M
a	m	Length of the lubricant wedge (Figure 1), equation (5)
$\alpha - \alpha_0$	rad	Reduction-tube-diameter angle (Figure 1)
α_0	rad	Tube-wall deformation angle (Figure 1)
α^*_0	rad	Characteristic angle added to ε^*_0
v_R	m/s	Circumferential roll speed
v_C	m/s	Tube speed
v_T	m/s	Mandrel speed
$d_T/2$	m	Mandrel radius
R	m	Stand-roll radius
R_0	m	$R_0 = R + S_{CX}$
S_C	m	Tube-wall thickness on the mandrel after the deformation zone
S_{C1}	m	Rolled-tube wall thickness
L_R	m	Abscissa projection of the tube-diameter-reduction zone
L_S	m	Abscissa projection of the tube-wall-projection zone
L_D	m	$L_D = L_R + L_S$
τ_x	Pa	Tangential stress in the lubricant layer
	Pa s	Dynamic lubricant viscosity under rolling pressure
η_0	Pa s	Dynamic lubricant viscosity under atmospheric pressure
u	m/s	Lubricant speed along the abscissa
γ	Pa ⁻¹	Lubricant-viscosity piecoefficient
p	Pa	Rolling pressure
Q	m ² /s	Lubricant use on the mandrel perimeter: one-dimensional model
dp/dx	Pa/m	Pressure gradient in the lubricant layer, equation (2)
$\partial p/\partial x$	Pa/m	Partial-pressure differential along the abscissa, equation (1)
$\sin\alpha...$ $\ln(\varepsilon_a)$	rad...	Symbol for the trigonometric functions and natural logarithm
		Symbols for the viewing locations of the AutoCAD cameras. After the approximate calculations according to Table 2 the obtained data are compared to the numerical Monte-Carlo solutions obtained with the mathematical programs and then modelled with AutoCAD, Figures 6 and 7 .
Ψ	m	Rolling-line zone described with the solutions from Table 1 and Figure 3 , according to ^{4,5} , for the lubricant surplus on the mandrel.
Ω	m	Rolling line after the Ψ zone where ε_a influences ε_0 and the solutions are presented, in this work, as the zone of tube-diameter reduction.

Σ	m	Part of the rolling line with the start and finish of intensive lubricant pickling on the mandrel and in the place where a tube-wall deformation takes place.
Φ	m	Area around point M from Figure 3 where interpolation polynomials can be used to connect the lubricant-layer calculations with the Ω and Σ equations from Table 1 .
$\Omega - I$	m	Larger area around point M, shown in Figure 9 and suitable for using the polygonal method ¹⁴
M-Point	m	Point of the approximate analytical solution from Table 1 controlling the numerical Monte-Carlo method, allowing a linear correction of the lubricant layer in Figure 8b . The effect is noticeable in Figures 3 and 5 .
W	-	Reference point in Figure 3 ; right of W – reduction of the tube diameter; left of W – deformation of the tube wall. It explains the topics and has no analytical expression.
$\gg, \approx, ^0, \rightarrow, \wedge, E$	-	Mathematical symbols for much greater, approximate, step mark, tending, mark for an exponent, base of number 10
A	m ⁻¹	Technological parameter: $A = [1 - \exp(-p)] / [6 \cdot (v_C + v_T)]$
\exp^{16}	-	Base of natural logarithm, a reference

5 REFERENCES

- I. Mamuzić, V. M. Drujan, Teorija, Materijali, Tehnologija Čeličnih cijevi, Hrvatsko Metalurško Društvo, Zagreb 1996, 137–275
- S. V. Mazur, Postanovka zadači i zakonomernosti tečenja smazki v očage deformaciji pri prokatke trub, Sučasni problemi metalurgii, Nacionalna Metallurgičeskaja Akademia Ukraine, Dnepropetrovsk, Ukraine, 8 (2005), 447–452
- D. Čurčija, I. Mamuzić, Mater. Tehnol., 39 (2005) 3, 61–75
- O. P. Maksimenko, A. A. Semenča, Issledovanie kontaktno-gidrodinamičeskoj smazki pri prokatke, Sučasni problemi metalurgii, Nacionalna Metallurgičeskaja Akademia Ukraine, Dnepropetrovsk, Ukraine, 8 (2005), 99–103
- P. L. Klimenko, Kontaktnije naprjaženija pri prokatke s tehnologičeskoj smazkoj, Sučasni problemi metalurgii, Nacionalna Metallurgičeskaja Akademia Ukraine, Dnepropetrovsk, Ukraine, 8 (2005), 44–49
- D. Čurčija, Mater. Tehnol., 37 (2003) 5, 237–250
- D. Čurčija, I. Mamuzić, Metalurgija, 44 (2005), 221–226
- D. Čurčija, I. Mamuzić, Metalurgija, 44 (2005), 295–300
- D. Čurčija, I. Mamuzić, Lubricating film shape at band dressing, 38th Symposium Lubricants, Zagreb, Društvo za Goriva i Maziva, Rovinj, Croatia, 2005
- D. Čurčija, I. Mamuzić, Metalurgija, 43 (2004), 249
- D. Čurčija, I. Mamuzić, Goriva i Maziva, 46 (2007), 34–44
- D. Čurčija, I. Mamuzić, F. Vodopivec, Metalurgija, 45 (2006), 250
- D. Čurčija, I. Mamuzić, Mater. Tehnol., 41 (2007) 1, 21–27
- D. Čurčija, I. Mamuzić, Tehnika RGM, 34 (1983), 1075–1078
- D. Čurčija, I. Mamuzić, Estimation of lubricant film by pipe rolling in stands/mills, 40th Scientific Symposium Lubricants 2007, Pula, Croatia, 2007
- D. Čurčija, I. Mamuzić, Mater. Tehnol., 42 (2008) 2, 59–63